LA-UR- 97-906

CONF-970944--7

Title:

INFLUENCE OF TWINNING ON THE CONSTITUTIVE RESPONSE OF Zr: EXPERIMENTS AND MODELING

Author(s):

Shuh Rong Chen and George T. Gray III

Materials Science and Technology Division
Los Alamos National Laboratory
Los Alamos, NM 87545

To be presented and published in:

DYMAT 97
International Conference on Mechanical and Physical Behavior of Materials Under Dynamic Loading
September 22-26, 1997
Toledo, SPAIN

MASTER

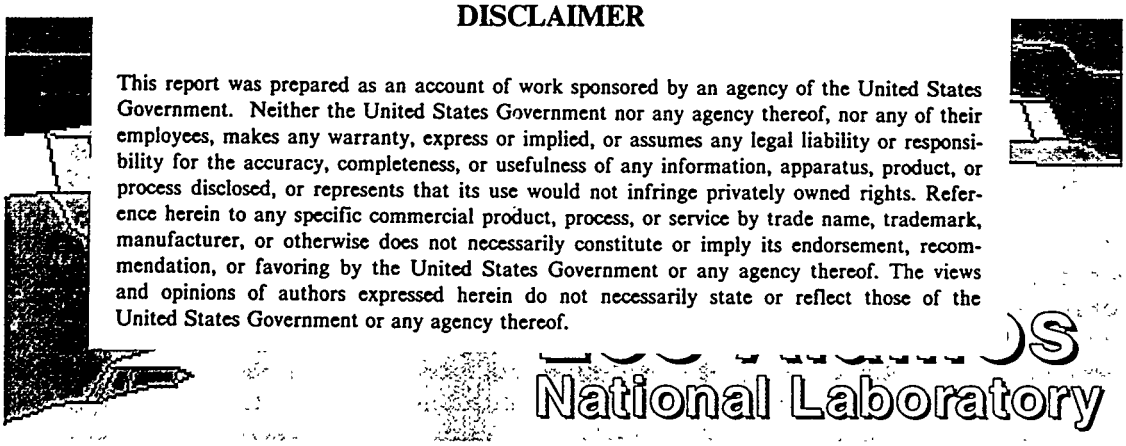

Influence of Twinning on the Constitutive Response of Zr: Experiments and Modeling

Shuh Rong Chen and George T. (Rusty) Gray III

Materials Science and Technology Division
Los Alamos National Laboratory
Los Alamos, NM 87545, USA

Abstract: The stress-strain response of Zr due to twinning is distinctly different from that due to slip as a function of temperature and strain rate. When the applied stress is lower than the transition stress, dislocation slip is the dominant deformation mechanism. The traditional MTS model is shown to adequately represent the constitutive behavior of Zr. Above the transition stress twinning becomes the dominant deformation mechanism where the flow stress increases linearly with strain. In this regime the rate-dependent strain hardening can be described by equations based on thermal activation theory that are very similar to the formula used in the MTS model.

Résumé: Le maclage du zirconium induit une réponse mécanique, en fonction de la température et de la vitesse déformation, bien distincte de celle produite par glissement. Quand la contrainte appliquée est inférieure à la contrainte de transition, le glissement est le mécanisme de déformation prépondérant. Le modèle MTS 'classique' décrit alors correctement le comportement viscoplastique du zirconium. Au dessus de la contrainte de transition, le maclage devient le mode de déformation dominant; la contrainte d'écoulement croît linéairement en fonction de la déformation. Dans ce régime, le comportement peut être décrit par des équations, fondées sur des lois d'activation thermique, similaires à celles utilisées dans le modèle MTS.

1. INTRODUCTION

The mechanical behavior of a pure Zr under quasi-static deformation at various temperatures has been investigated by Song and Gray recently [1]. The microstructure and the underlining deformation mechanisms were studied using optical and transmission electron microscopy. Several conclusions were derived from their study: (1) The rate-controlling deformation mode under compression was seen to change from twinning at low temperatures to slip at elevated temperatures, (2) The transition from slip control to twinning control takes place when the flow stress is higher than a critical stress for uniform twinning to occur, and (3) The stress-strain response due to twinning is distinctly different from that due to slip. A moderate but persistent work hardening rate is associated with twinning. The objective of this paper is to construct a physically-based constitutive model to describe these processes and extend the stress-strain studies to high-rate deformation.

2. EXPERIMENTAL PROCEDURE

The material studied in this investigation was crystal-bar high-purity zirconium. The metal was supplied in the form of 45-mm-diameter bar stock. A cylinder, 45-mm diameter by 56 mm, of the crystal-bar Zr stock was upset and clock-rolled at room temperature with two intermediate anneals (600°C for 1 hour and 1/2 hour after upsetting and 50% rolling reduction, respectively). This rolling and annealing schedule produced a strong in-plane isotropic basal texture in the plate; the (0002) plane normals lying nominally 20 degrees inclined to the plate surface.

Cylindrical specimens, 5-mm height and 5-mm diameter, were machined from the rolled Zr plate in the through-thickness direction. The samples were given a final anneal at 600°C for 2 hours to yield a fully recrystallized structure with an equiaxed grain size of 25 μm. Specimens were compressed quasi-statically at strain rates of 10^{-1} and 10^{-3} s^{-1} at various temperatures (from 77 to 956 K). Dynamic tests were conducted as a function of strain rate, 1000-6000 s^{-1}, at 77 and 298 K, utilizing a Split-Hopkinson Pressure Bar [2].

3. RESULTS AND DISCUSSION

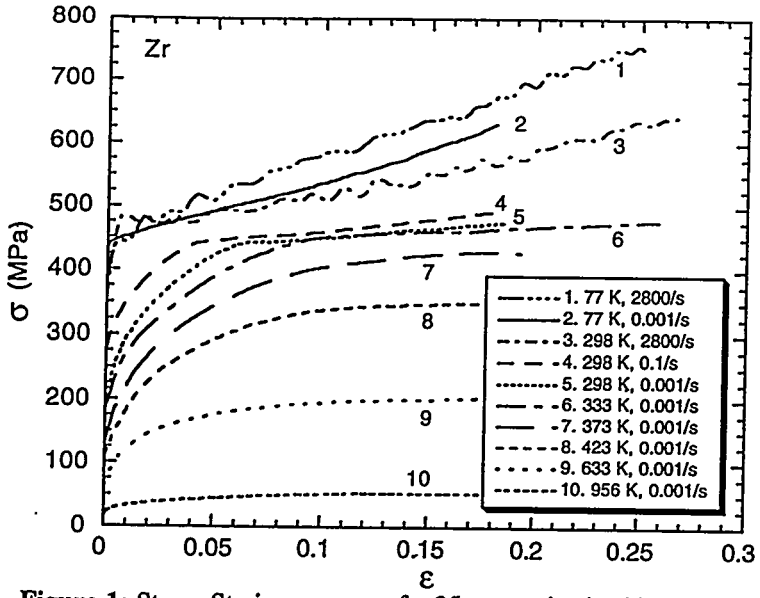

Figure 1: Stress-Strain response of a 25 μm grain size high-purity Zr as a function of temperature and strain rate.

Stress-Strain Response: The stress-strain responses of high-purity-Zr deformed both quasi-statically from 77 to 956 K and dynamically at 77 and 298 K are shown in Fig. 1. The yield stresses exhibit very high temperature and strain rate sensitivity that are typical for bcc and hcp metals. The strain hardening rate ($d\sigma/d\varepsilon$) is also seen to depend strongly on the temperature and strain rate. There are three distinct types of stress-strain behavior shown in Fig. 1. For the curves labeled 1, 2, and 3 which correspond to dynamic deformation at low temperature or quasi-static compression at 77 K, the stresses at the initiation of plastic deformation are essentially the same. The strain hardening rate is nearly a constant but depends on the deformation temperature and strain rate. Metallographic examination[1] confirmed that in this regime (referred to as stage "T") twinning is the dominant deformation mechanism. Above 373 K at low strain rate (curves labeled 7, 8, 9, and 10), Zr yields smoothly and the stress-strain curves gradually level off leading to a saturation stress where the rate of work hardening due to dislocation generation is balanced by the rate of dynamic recovery resulting from dislocation annihilation. The saturation stress is a strong function of temperature (and strain rate). This regime will be referred to as stage "S" for slip. Samples deformed between 298 K and 333 K (curves labeled 4, 5, and 6), however, show a rather different pattern. Similar to the higher temperature tests, at these rates and temperatures they yield smoothly and exhibit a continuous decrease in work-hardening rate. At a certain strain, the gradually decreasing strain-hardening rate turns discontinuously into a nearly constant but lower value, indicative of a change in the rate-controlling deformation mode.

The transition from stage T to stage S was analyzed previously [1]. It was concluded that the transition stress ($\sigma_{twin.stress}$) is insensitive to temperature and was found to be about 440 MPa. The transition strain ($\varepsilon_{twin.strain}$) was the strain value corresponding to the $\sigma_{twin.stress}$ and was found to be temperature and strain rate dependent.

Constitutive Modeling: The Mechanical Threshold Stress (MTS) model is used in this study to analyze the constitutive response of Zr. The framework and details of the MTS model have been given previously [3-6]. The MTS model functional form is given here for completeness,

$$\frac{\sigma}{\mu} = \frac{\sigma_a}{\mu} + S_i(\dot{\varepsilon},T)\frac{\hat{\sigma}_i}{\mu_0} + S_\varepsilon(\dot{\varepsilon},T)\frac{\hat{\sigma}_\varepsilon}{\mu_0} \qquad (1)$$

$$S_i(\dot{\varepsilon},T) = \left\{1-\left[\frac{kT}{\mu b^3 g_{0i}}\ln\left(\frac{\dot{\varepsilon}_{0i}}{\dot{\varepsilon}}\right)\right]^{1/q_i}\right\}^{1/p_i} \qquad (2)$$

$$S_\varepsilon(\dot{\varepsilon},T) = \left\{1-\left[\frac{kT}{\mu b^3 g_{0\varepsilon}}\ln\left(\frac{\dot{\varepsilon}_{0\varepsilon}}{\dot{\varepsilon}}\right)\right]^{1/q_\varepsilon}\right\}^{1/p_\varepsilon} \qquad (3)$$

$$\frac{d\hat{\sigma}_\varepsilon}{d\varepsilon} = \theta_0\left[1-F\left(\frac{\hat{\sigma}_\varepsilon}{\hat{\sigma}_{\varepsilon s}}\right)\right] \qquad (4)$$

$$F\left(\frac{\hat{\sigma}_\varepsilon}{\hat{\sigma}_{\varepsilon s}}\right) = \frac{\tanh(\alpha\hat{\sigma}_\varepsilon/\hat{\sigma}_{\varepsilon s})}{\tanh(\alpha)} \qquad (5)$$

$$\frac{\hat{\sigma}_{\varepsilon s}}{\hat{\sigma}_{\varepsilon s0}} = \left(\frac{\dot{\varepsilon}}{\dot{\varepsilon}_{0\varepsilon s}}\right)^{kT/\mu b^3 g_{0\varepsilon s}} \qquad (6)$$

Plastic deformation is known to be controlled by the thermally activated interactions of dislocations with obstacles. The flow stress is separated into athermal (σ_a) and thermal components (the second and third terms on the right-hand side of Eq. (1)). In the MTS model, the current structure of a material is represented by an internal state variable, the mechanical threshold ($\hat{\sigma}(\hat{\sigma}_i,\hat{\sigma}_\varepsilon,..)$), which is defined as the flow stress at 0 K. The function in Eq. (2) and (3) specifies the ratio between the applied stress ($\sigma(\sigma_i,\sigma_\varepsilon,..)$) and the mechanical threshold stress for a given type of obstacle at a constant structure in the thermally activated glide regime. The second term on the right-hand side of Eq. (1) describes the

rate-dependent portion of the yield stress. The third term on the right-hand side of Eq. (1) describes the structure evolution with strain. A phenomenological relation describing the hardening behavior is represented by Eq. (4) and (5) with a rate dependent saturation stress ($\hat{\sigma}_{es}$). A power law is used to relate this saturation stress to the temperature and strain rate (Eq. (6)). A temperature dependent shear modulus in the form of $\mu = \mu_0 - D/[\exp(T_0/T) - 1]$ is used [7]. Above 900 K the shear modulus changes abruptly which is linked to the hcp->bcc transformation [8].

The contribution to the flow stress arising from different obstacles has to be examined to achieve a physically based modeling fit. The athermal stress can be rationalized as the yield stress obtained at very high temperature. A value of 5 MPa is chosen for Zr. The second term on the right-hand side of Eq. (1) represents the thermal contribution to the yield stress on top of the athermal contribution. It is further assumed that it does not evolve with strain. In well-annealed materials, the initial dislocation density is low enough so that the contribution from the strain-hardening term at very low strains can be neglected. From the plot (Fig. 2) of the yield stress (σ_y) as a function of the normalized activation energy (combining temperature and strain rate into a single variable, $G_{norm} = [kT/\mu b^3 \cdot \ln(\dot{\varepsilon}_{0i}/\dot{\varepsilon})]^{1/q_i}$), the corresponding parameters which describe the deviation from the mechanical threshold ($\hat{\sigma}_i$) as a function of temperature and strain rate can be determined. There are three distinct regimes as shown in Fig. 2. At low G_{norm} corresponding to twinning being the dominant deformation mode, the "yield" stress is a constant. Thermal activation theory is closely obeyed at higher G_{norm} with a high rate sensitivity of the yield stress at an intermediate range of G_{norm}, and a much lower rate-dependency of the yield stress at high temperatures. g_{0i} and $g_{0\varepsilon}$ in Eq. (2) and (3) are the normalized total activation energies for dislocations to overcome the different obstacles. The common values are between 0.1 and 2 with a value smaller than 0.5 being termed as highly rate dependent and a value close to 1 reflecting a low rate dependency. Within the intermediate range of G_{norm}, g_{0i} is relatively small (0.267). This small value of the normalized total activation energy suggests that the rate-controlling mechanism in Zr is overcoming the Peierls barrier, which has a small activation volume [9,10]. The demarcation value of G_{norm}, above which the Peierls stress is no longer the rate-controlling mechanism is not precisely determined. Additional high temperature/lower strain-rate experiments are needed if the application is within the high G_{norm} regime.

A typical feature of the curves in Fig. 1, where dislocation slip is the deformation mode, is that they diverge: the rate and temperature dependence appears to be greater at large strains than at small strains. This divergence is primarily an effect of the influence of thermal activation on the rate of substructure evolution, i.e. strain hardening. Fig. 3 exhibits the data for two of the temperatures in Fig. 1 on a diagram of hardening rate $\theta \equiv (d\sigma/d\varepsilon)_{T,\dot{\varepsilon}}$ versus stress σ. The hardening rate always decreases starting from the beginning of the tests. The appropriate value of α in Eq. (5) that describes the way the material approaches saturation, can be determined from this hardening curve. It is further observed that at ~440 MPa the hardening rate changes suddenly to a lower and almost constant value. This hardening rate, which reflects where twinning becomes the deformation mode, is rate dependent as shown in Fig. 3.

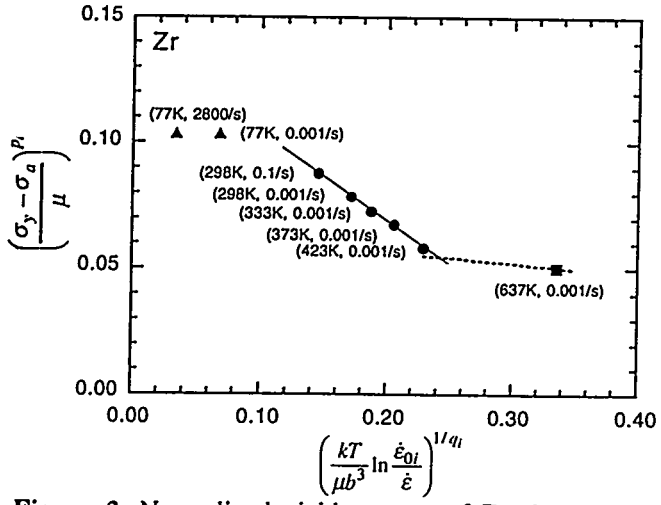

Figure 2: Normalized yield stresses of Zr plotted vs. normalized activation energies.

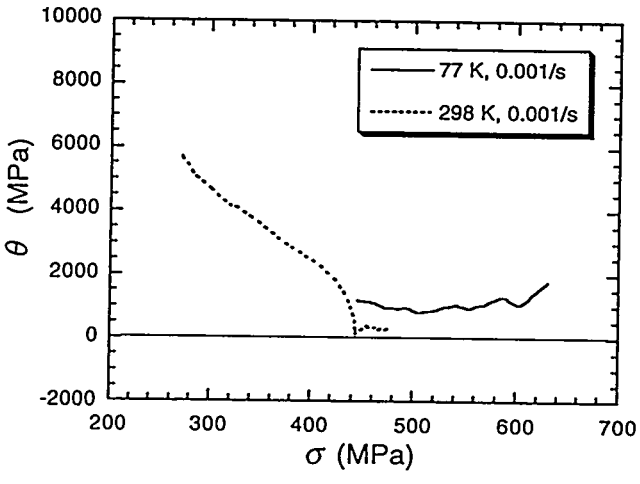

Figure 3: Strain hardening curves of Zr compressed quasi-statically at 77 and 298K.

For each $\sigma(\varepsilon)$ curve, a corresponding mechanical threshold $\hat{\sigma}_\varepsilon(\varepsilon)$ describing the structural evolution after yielding is derived according to:

$$\hat{\sigma}_\varepsilon(\varepsilon) = \frac{\mu_0}{S_\varepsilon}\left(\frac{\sigma(\varepsilon)}{\mu} - \frac{\sigma_a}{\mu} - S_i\frac{\hat{\sigma}_i}{\mu_0}\right) \tag{7}$$

The constants used in the S_ε factor were $\dot{\varepsilon}_{0\varepsilon} = 10^7\ s^{-1}$, $g_{o\varepsilon}$ =1.6, p_ε =2/3, and q_ε =1, with $g_{o\varepsilon}$ being the more critical parameter, based on previous experience with Cu [3] and other materials [4,5]. Eq. (4) an (5) are then used to fit to $\hat{\sigma}_\varepsilon(\varepsilon)$ with an initial hardening rate θ_0 and the saturation stress $\hat{\sigma}_{\varepsilon s}$ as the adjustable parameters for each test condition. The initial hardening rate normalized by the shear modulus as a function of temperature and strain rate is plotted in Fig. 4. It is seen that a constant normalized initial hardening rate is adequate to unify the parameter θ_0. The rate dependent $\hat{\sigma}_{\varepsilon s}$ is given in Fig. 5 according to Eq. (6). The saturation stress decreases at higher temperatures or low strain rates due to a higher rate of dynamic recovery under these testing conditions.

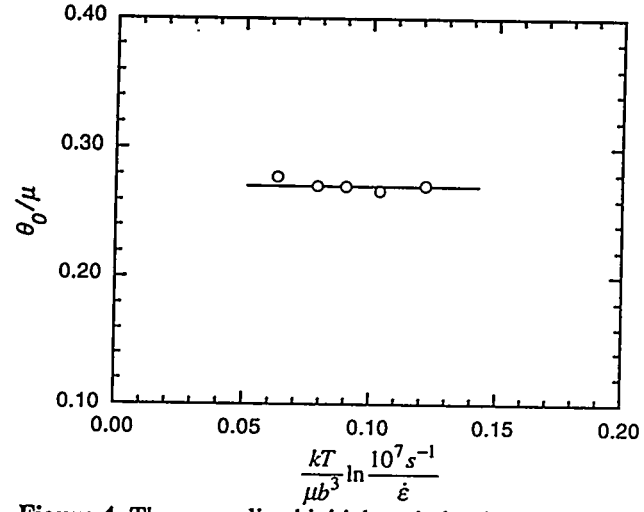

Figure 4: The normalized initial strain hardening rate as a function of temperature and strain rate in the regime where dislocation slip is the dominant deformation mode.

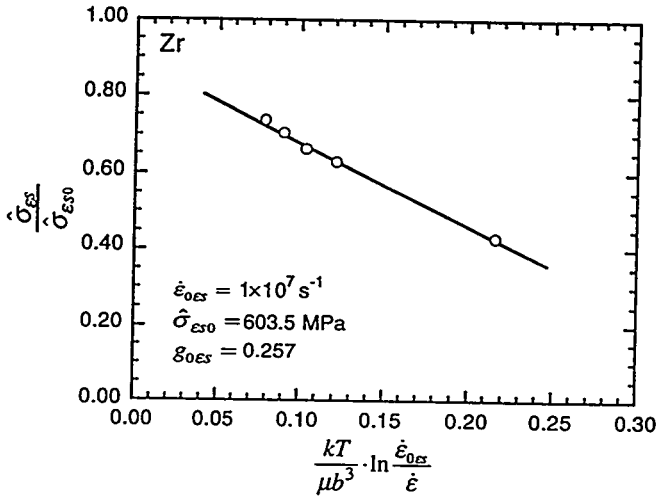

Figure 5: Saturation stresses at 0 K of Zr that were plotted versus temperature and strain rate according to Eq. (6).

Based on the analysis above, the model-fitting results for Zr are shown in Fig. 6. The traditional MTS model, which utilizes linear addition of an athermal component to thermal components consisting of descriptions of the yield stress and structure evolution, is shown to adequately represent the constitutive behavior of Zr in the regime where dislocation slip is the dominant deformation mechanism. The calculation is much higher than the experimental data at 77 K and at higher strains at 298 K where twinning becomes the dominant deformation mechanism. The increase in the Peierls stress barrier to dislocation movement with decreasing temperature due to the reduction of thermal activation is the primary reason why pure Zr yields or deforms by twinning rather by slip at lower temperatures. The other reason is that twinning is favored due to the shear stresses applied in the through-thickness plate loading direction for these samples requiring substantial c-axis contraction during compression due to the strong basal texture of the plate.

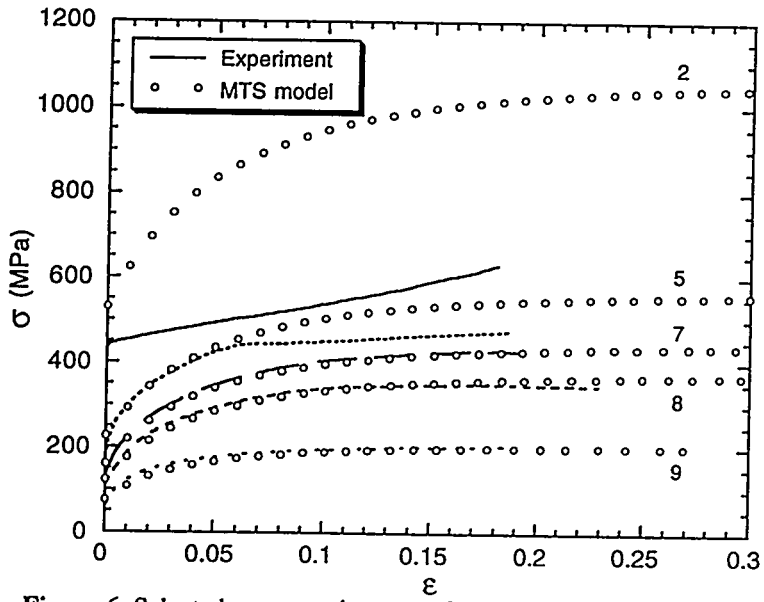

Figure 6: Selected stress-strain curves for Zr showing the fit to the MTS model as the open circles. The model fit is calculated assuming dislocation slip is the dominant deformation mechanism for the whole temperature and strain rate regime. Same label numbers for the curves as in Fig. 1 are used.

When the applied stress is higher than the transition stress either at yield

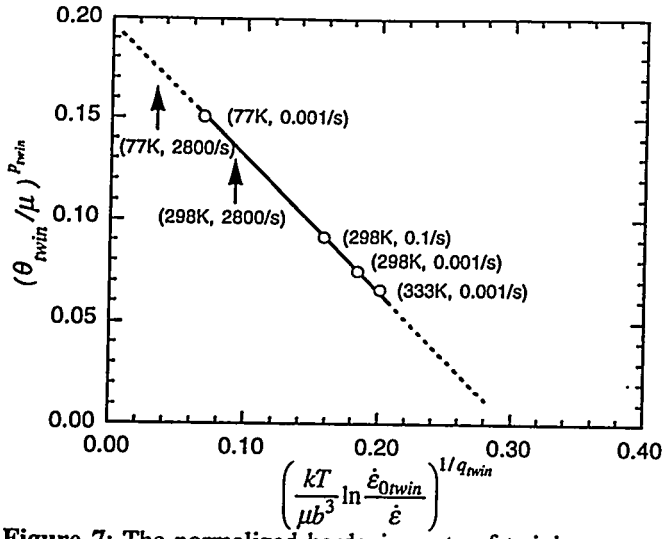

Figure 7: The normalized hardening rate of twining as a function of temperature and strain rate in the regime where twinning is the dominant deformation mode.

(77 K) or after a certain strain, the flow stress increases linearly with strain (i.e., the strain hardening rate is nearly a constant). The strain hardening rate of twinning is rate dependent which has been shown in Fig. 3. At the time this analysis was done, dynamic compression data were not available. The hardening rates measured from hardening curves when twinning was the dominant deformation mode were 925, 300, 200, and 150 MPa under the four test conditions labeled associated with the data points in Fig. 7. It is obvious that the hardening rate of twinning θ_{twin} decreases much faster as a function of temperature than the change of shear modulus versus temperature, otherwise Fig. 7 will be similar to Fig. 4. Therefore the relation of θ_{twin} as a function of temperature and strain rate based on a thermal activation process is proposed to fit to the data. The overall fit (solid line) as shown in Fig. 7 is satisfactory based on the limited number of test results. It is seen that θ_{twin} is strongly rate dependent with a g_{0twin} of 0.16463. The dynamic tests at 77 K will fall in the low normalized activation energy that is outside the curve fit while the one at 298 K will fall inside the normalized activation energy measured (indicated by arrows in Fig. 7). These two extra experiments will be used to verify the validity of the extrapolation and the interpolation of the model that is mainly based on thermal activation theory. The following equations are used when twinning is the dominant deformation mechanism:

For $\sigma \geq \sigma_{twin.stress}$: $\quad \varepsilon_{twin.strain} \Leftrightarrow \sigma_{twin.stress}$

$$\frac{\sigma}{\mu} = \frac{\sigma_{twin.stress}}{\mu} + S_{twin}(\dot{\varepsilon},T)\cdot\frac{\hat{\sigma}_{twin}}{\mu_0} = \frac{\sigma_{twin.stress}}{\mu} + S_{twin}(\dot{\varepsilon},T)\cdot\frac{\hat{\theta}_{twin}\cdot(\varepsilon-\varepsilon_{twin.strain})}{\mu_0} \tag{8}$$

$$S_{twin}(\dot{\varepsilon},T) = \left\{1-\left[\frac{kT}{\mu b^3 g_{0twin}}\ln\left(\frac{\dot{\varepsilon}_{0twin}}{\dot{\varepsilon}}\right)\right]^{1/q_{twin}}\right\}^{1/p_{twin}} \tag{9}$$

Final model-fitting results encompass both dislocation slip and deformation twinning mechanisms are shown in Fig. 8. Parameters and their values for the MTS model for Zr are listed in Table I. The stress-strain calculations follow the experimental data closely for the regime where dislocation slip is the dominant deformation mode. Above a critical twinning stress, corresponding to the nucleation of twinning embryos, the material starts to deform by twinning. The hardening due to twinning is caused by the increase of the number of twins per unit volume and the thickening of these existing twins [1]. The thickening of the twins leads to strain hardening since the mismatch of the coherent twin boundary is linearly proportional to the thickness of the twins [11]. The increase in the number of twins also decreases the effective grain size and thereby increases the applied stress necessary to initiate new twins. The model "*prediction*" for two dynamic tests at 77 K (curve 1) and at 298 K (curve 3) in Fig. 8 are very good. The number of twins and their thickness both

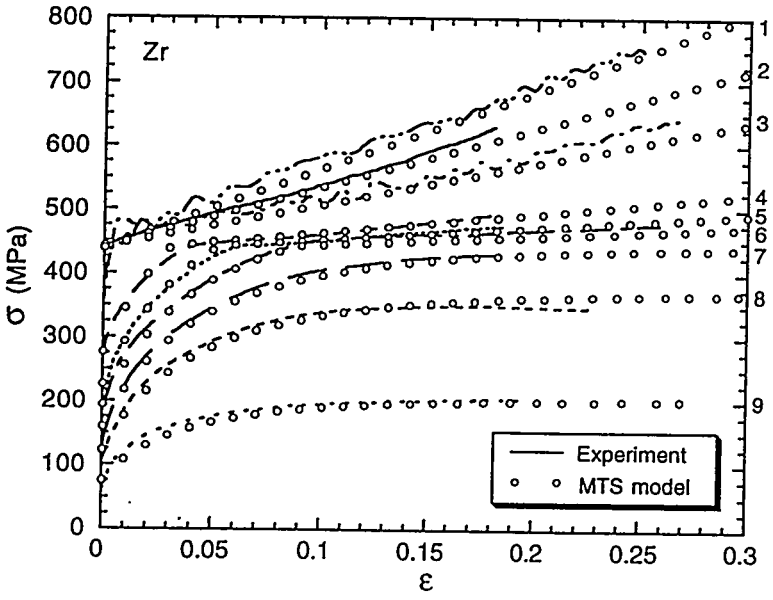

Figure 8: Stress-strain curves of Zr showing the fit to the MTS model as the open circles. The model fit is calculated when dislocation slip is the dominant deformation mechanism below the critical twinning stress, and twinning becomes the dominant deformation mode above the critical twinning stress. The same label numbers for the curves as in Fig. 1 are used.

decrease as a function of temperature and strain rate as evidenced from previous microstructural studies [11] that lead to lower work hardening rates at higher temperature.

It has been shown that the yield and apparent twinning stresses strongly depend on the grain size [1,12]. The yield (or twinning) stress for Zr at 77 K at 10^{-3} s^{-1} for a grain size of 25 μm is 440 MPa while it is 220 MPa for a grain size of 75 μm. Tests under dynamic conditions at 77 K and 298 K show a similar influence of grain size on flow stress. The texture effect on the stress was investigated by compressing samples transversely for an Alpha-Ti [12]. The transverse direction has a softer orientation for slip to occur such that the flow stress is lower than the one compressed in the through thickness direction. A similar study is underway for Zr. The deformation mechanisms may be a mixture of slip and twinning at lower temperatures or under higher strain rates. The grain-size effect, the anisotropy of the material due to processing and its effects on the stress-strain behavior as well as the change of deformation characteristics in Zr, are being studied systematically. Work on the construction of a physically-based constitutive model to include both twinning and slip will continue.

Table I. Parameters for Zr for the MTS Model

Parameter	Value	Unit	Parameter	Value	Unit	Parameter	Value	Unit
μ_0	41762	MPa	p_i	1/2	-	p_ε	1/2	-
D	1999	MPa	if $[kT/\mu b^3 \cdot \ln(\dot{\varepsilon}_{0i}/\dot{\varepsilon})]^{1/q_i} < 0.24$			$\hat{\theta}_{twin}$	1580	MPa
T_0	85.038	K	g_{0i}	0.26676	-	$\dot{\varepsilon}_{0\varepsilon s}$	1×10^7	s^{-1}
b	3.23×10^{-10}	m	$\hat{\sigma}_i$	750.5	MPa	$\hat{\sigma}_{\varepsilon s0}$	603.5	MPa
σ_a	5	MPa	if $[kT/\mu b^3 \cdot \ln(\dot{\varepsilon}_{0i}/\dot{\varepsilon})]^{1/q_i} \geq 0.24$			$g_{0\varepsilon s}$	0.257	
$\sigma_{twin.stress}$	442	MPa	g_{0i}	1.0	-	$\dot{\varepsilon}_{0twin}$	1×10^7	s^{-1}
θ_0/μ	0.2716	-	$\hat{\sigma}_i$	238.8	MPa	g_{0twin}	0.16463	-
α	1	-	$\dot{\varepsilon}_{0\varepsilon}$	1×10^7	s^{-1}	q_{twin}	3/2	-
$\dot{\varepsilon}_{0i}$	1×10^6	s^{-1}	$g_{0\varepsilon}$	1.6	-	p_{twin}	1/2	-
q_i	3/2	-	q_ε	3/2	-			

4. CONCLUSIONS

Based upon a study of temperature and strain rate on the structure/property response of high-purity zirconium, the following conclusions can be drawn: (1) there exists a critical transition stress that demarcates the deformation mechanisms of dislocation slip and twinning, (2) in the dislocation slip regime, the traditional MTS model is shown to adequately represent the constitutive behavior, (3) when twinning becomes the dominant deformation mechanism the strain hardening rate as a function of temperature and strain rate can be described by equations based on thermal activation theory that are very similar to the formula used in the original MTS model describing slip.

Acknowledgments

This work was supported under the auspices of the United States Department of Energy. The authors acknowledge the assistance of M.F. Lopez and Robert W. Carpenter II for conducting the quasi-static and high-strain-rate mechanical testing.

References

1. S.G. Song and G.T. Gray, III: *Metall. Trans. A*, 1995, vol. 26A, pp. 2665-2675.
2. P.S. Follansbee: *High Strain Rate Compression Testing - The Hopkinson Bar,* 9th edn. Vol. 8, Am. Soc. Metals, Metals Park, Ohio, 1985, pp. 198-203.
3. P.S. Follansbee and U.F. Kocks: *Acta metall.*, 1988, vol. 36, pp. 81-93.
4. P.S. Follansbee and G.T. Gray, III: *Metall. Trans. A*, 1989, vol. 20A, pp. 863-874.
5. P.S. Follansbee, J.C. Huang, and G.T. Gray, III: *Acta metall.*, 1990, vol. 38, pp. 1241-1254.
6. S.R. Chen and G.T. Gray, III: *Metall. Trans. A*, 1996, vol. 27A, pp. 2994-3006.
7. Y.P. Varshni: *Phys. Rev. B*, 1970, vol. 2, pp. 3952-3958.
8. E.S. Fisher and C.J. Renken: *Phys. Rev.*, 1964, vol. 135, pp. A482-A494.
9. K.G. Hoge and A.K. Mukherjee: *J. Mater. Sci.*, 1977, vol. 12, pp. 1666-1672.
10. H. Conrad: *J. Metals*, 1964, vol. 16, pp. 582-588.
11. S.G. Song and G.T. Gray, III: *Acta metall. mater.*, 1995, vol. 43, pp. 2325.
12. G.T. Gray, III: *DYMAT 97*, in this volume.